Organic LETTERS

Letter

pubs.acs.org/OrgLett

Synthesis and Electronic Structure of Dicyanofulvene-Fused Electron Accepting Molecule Based on a 1,5-Dihydro-*s*-Indacene Framework

Yasutaka Endo,[†] Masashi Hasegawa,*[,†] Tamami Matsui,[‡] Hajime Yagi,[‡] Shojun Hino,[‡] and Yasuhiro Mazaki*[,†]

[†]Department of Chemistry, Graduate School of Science, Kitasato University, 1-15-1 Kitasato, Minami-ku, Sagamihara, Kanagawa 252-0373, Japan

[‡]Department of Applied Chemistry, Graduate School of Engineering, Ehime University, 3 Bunkyocho, Matsuyama, Ehime 790-8577, Japan

Supporting Information

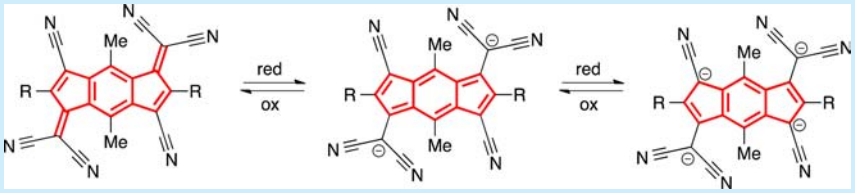

ABSTRACT: A novel dicyanofulvene dimer fused to a benzene ring (**3a**) has been synthesized as an electron-accepting molecule. The low-lying LUMO level was validated by measuring the ultraviolet photoelectron spectroscopy and electronic spectra. Cyclic voltammetry exhibited sequential reversible waves from **3a** to $\mathbf{3a}^{4-}$ in a range of −0.30 to −2.14 V (vs Fc/Fc^{+}). The electronic structure of **3a** and its anionic species ($\mathbf{3a}^{\bullet-}$, $\mathbf{3a}^{2-}$, $\mathbf{3a}^{3\bullet-}$, and $\mathbf{3a}^{4-}$) were investigated by electronic spectra and X-ray crystallographic analyses.

The design and synthesis of novel electron-depleted molecules has received considerable attention for their prospective use in electron transporting (n-type) materials, such as field-effect transistors (FET), dye-sensitized solar cells (DSCs), and electroluminescence (EL) materials.[1] While a wealth of electron-donating molecules have been synthesized so far, investigations of the electron-accepting molecules are relatively limited due to the instability of the anionic species and the difficulty of the preparation.[2] Therefore, exploration for a superior acceptor is an ongoing and intriguing research topic.

One efficient modification of the π-system with high electron affinity is the incorporation of unsaturated five-membered carbocycles.[3] They exhibit a proaromatic character that can lead to stable anionic species by facile reduction. Due to the antiaromatic 12π character, the *s*-indacene framework (**1**) meets the structural criteria.[4] Nevertheless, despite the adequate ability of the *s*-indacene framework, these compounds are highly reactive and difficult to isolate for material use. Therefore, these scaffolds are usually covered with steric substituents for kinetic stabilization or embedded into a (poly)cyclic conjugated system for resonance stabilization. In line with these strategies, a series of indenofluorene derivatives, which contain *s*-indacene moieties, have been intensively developed by several groups.[4−7] For instance, Haley et al. recently synthesized diethynyl substituted indeno[1,2-*b*]fluorene as an antiaromatic analogue of pentacene and investigated its electronic structure.[5d,6a] Yamashita et al. reported indeno[1,2-*b*]fluorene with aryl substituents for FET materials.[6b] In addition, the ladder-type structure of indeno[1,2-*b*]fluorene involving dicyanofulvene moieties (**2**) was synthesized as an acceptor for a charge-transfer (CT) complex.[8] More recently, Marks et al. prepared soluble ladder-type molecules and evaluated their electronic properties.[9] However, their reduction potential, which is associated with the LUMO level, is more negative than conventional quinodimethane derivatives such as the representative examples of TCNQ, TNAP, and others. Due to the strong aromatic stabilization, benzo-annulation from both sides might hamper the intrinsic reduction ability of the *s*-indacene core.

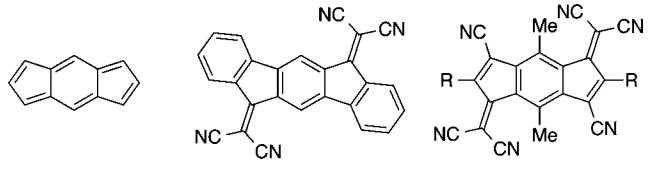

1 **2** **3a** (R = ^{n}Bu) **3b** (R = Me)

Therefore, we predict that a decrease in the benzo-annulation would improve the electron affinity. In addition, the removal of the benzene rings at the end of indenofluorene allows for further chemical modification of the *s*-indacene core. Thus, we designed a dicyanofulvene (DCF)[10] derivative (**3a**) that involves a 3,7-dicyano-1,5-dihydro-*s*-indacene moiety. It can be a novel electron-accepting molecule with a low-lying LUMO level because a defused DCF framework can be a superior electron

Received: September 10, 2014
Published: October 13, 2014

dx.doi.org/10.1021/ol502675n | *Org. Lett.* 2014, 16, 5608−5611

acceptor itself. The direct attachments of six nitrile groups can also accelerate the electron-accepting ability of the indacene core. Here, we report the synthesis of **3a** and its electrochemical properties as well as the electronic structure of its reduced form.

The synthesis of **3a** is summarized in Scheme 1. The treatment of the known tetrahydro-*s*-indacene-1,5-dione derivative **4**[11] with

Scheme 1. Synthesis of 3a

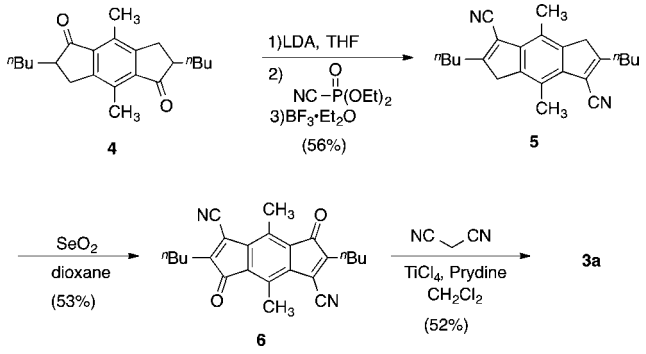

diethyl cyanophosphonate in the presence of LDA followed by the addition of $BF_3{\cdot}Et_2O$ gave the dicyano-substituted dihydro indacene **5** in 56% yield.[12,13] The oxidation of **5** with selenium dioxide afforded a purple needle of dicyanodione **6** in 53% yield. A condensation reaction between malononitrile and **6** in the presence of $TiCl_4$ and pyridine converted to **3a** in 52% yield. The molecular structure was characterized by ^1H, ^{13}C NMR, elemental analysis, IR, and UV−vis spectra together with X-ray crystallographic analysis.[14] This compound was obtained as a deep green crystal that was stable in both solution and the solid state.

Recrystallization of **3a** from a CH_2Cl_2−hexane solution gave a single crystal suitable for X-ray analysis (Figure 1). The molecule

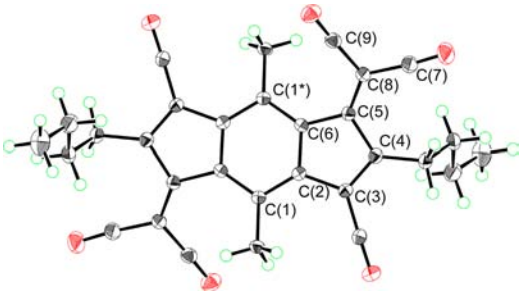

Figure 1. ORTEP drawing of **3a**. Selected bond lengths [Å]: C(1)−C(2) 1.398(2), C(2)−C(3) 1.476(2), C(3)−C(4) 1.361(2), C(4)−C(5) 1.485(2), C(5)−C(6) 1.479(2), C(6)−C(1*) 1.407(2), C(5)−C(8) 1.372(2).

was crystallized as monoclinic and $P2_1/c$, with a crystallographic inversion center at the benzene ring. The π-core of **3a** adopted a roughly planar form except for the $C(CN)_2$ moieties. The dihedral angle of C(6)−C(5)−C(8)−C(9) was 7.09°. Moreover, up-and-down deformation was found in $C{=}C(CN)_2$ moieties from the core. These noticeable distortions were due to the steric repulsion of CH_3 groups at the 4,8-positions, and it was also found in the optimized structure of **3b** by DFT calculation (B3LYP/6-311++G(d,p)).[15] In addition, the bond lengths of C(2)−C(3), C(4)−C(5), and C(5)−C(6) were slightly longer than the C_{sp^2}−C_{sp^2} bond length in the *s*-indacene core. In the packing motif, there was no significant contact between the intermolecular *s*-indacene cores while the C(7) in the CN substituent was close to other CN groups in the neighboring molecule.

In the electronic spectra, compound **3a** exhibited absorption bands at 292, 457 nm and a broad absorption band at 660 nm whose edge extended into the NIR region (Figure S5). In the theoretical prediction obtained from the TD-B3LYP/6-311++G(d,p) calculation for **3b**, the longest absorption was associated with the HOMO−LUMO transition in which the HOMO was mainly located in the *s*-indacene core and the LUMO was mainly located in the dicyanofulvene moieties (Figure 2). The longest absorption maxima of **5** and **6** were found at 318 and 540 nm, respectively, and hence, a pronounced reduction in the LUMO energy of **3a** was achieved (Figure S5).

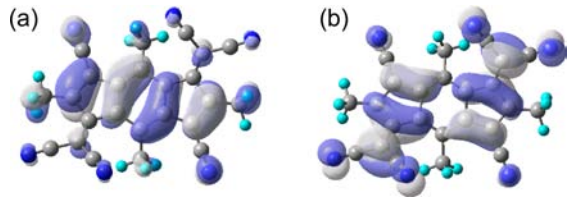

Figure 2. Molecular orbitals of **3b** (a) HOMO and (b) LUMO.

The ultraviolet photoelectron spectra of **3a** revealed the binding energy of the HOMO to be 7.7 eV and the threshold energy (E_{th}) to be 7.0 eV (Figure S8). Since the HOMO−LUMO energy gap estimated from the absorption spectrum (Figure S5) was 1.9 eV (660 nm), the LUMO level might be at least 1.9 eV above the HOMO level, namely 5.8 eV below the vacuum level. The optically obtained HOMO−LUMO gap is usually estimated to be slightly narrower than the gap obtained by electron spectroscopy or conduction measurements.[16] The actual LUMO level may be slightly higher than −5.8 eV.

Cyclic voltammetry (CV) analysis of **3a** was performed in THF containing Bu_4NPF_6 and compared to CV analyses for **5** and **6** (Table 1). Figure 3 shows the cyclic voltammogram of **3a**

Table 1. Redox Potentials of 3a, 5, and 6[a]

compd	$E^1_{1/2}$ (V)	$E^2_{1/2}$ (V)	$E^3_{1/2}$ (V)	$E^4_{1/2}$ (V)
3a	−0.30 (1e$^-$)	−0.76 (1e$^-$)	−1.65 (1e$^-$)	−2.14 (1e$^-$)
5	−1.33[b] (1e$^-$)	−1.67[b] (1e$^-$)	–	–
6	−0.88 (1e$^-$)	−1.58 (1e$^-$)	–	–
2[c]	−0.50 (1e$^-$)	−0.73 (1e$^-$)	−1.28 (1e$^-$)	−1.70 (1e$^-$)

[a]All potentials were obtained from CV measurements in THF containing 0.1 M ^{n}Bu$_4$NPF$_6$ at 25 °C with a glassy carbon working electrode. Potentials were measured against a Ag/Ag$^+$ electrode and converted to the values vs Fc/Fc$^+$. [b]Irreversible peak. [c]E_{red} values. Data from ref 8 with conversion to Fc/Fc$^+$ assuming Fc/Fc$^+$ = 0.46 V in SCE.

in THF. Compound **3a** showed four pairs of reversible redox waves, and the peak currents of each redox wave all had similar degrees. Thus, all redox waves correspond to a single-electron transfer. A markedly positive shift of the first redox potential ($E^1_{1/2}$ = −0.30 V) was found in **3a** compared to that of **6** ($E^1_{1/2}$ = −0.88 V). Replacement of the ketone with dicyanomethylene groups increased the electron-accepting ability. In addition, the $E^1_{1/2}$ value of **3a** was more positive than that of the ladder-type indeno[1,2-*b*]fluorene (**2**) ($E^1_{1/2}$ = −0.50 V, converted to the value vs Fc/Fc$^+$), and the value comparable to that of TCNQ (E^1_{red} = −0.25) under similar conditions. This finding clearly

dx.doi.org/10.1021/ol502675n | *Org. Lett.* 2014, 16, 5608−5611

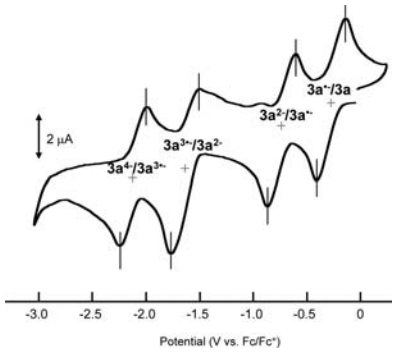

Figure 3. CV chart of **3a**.

indicated that the removal of the benzo-annulation and the introduction of CN groups contributed to the marked lowering of the LUMO level. In addition, two redox waves of $E^3_{1/2}$ and $E^4_{1/2}$ are assigned to the formation of $\mathbf{3a}^{3\bullet-}$ and $\mathbf{3a}^{4-}$, respectively.

To elucidate the electronic structures, spectroelectrochemistry of **3a** was performed in THF under an Ar atmosphere. We also carried out TD-DFT calculations (TD-(U)B3LYP) for **3b** as the model for **3a**. Figure 4 depicts the electronic spectra in each

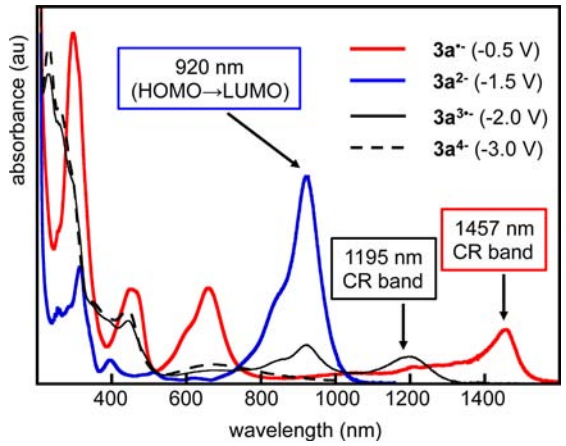

Figure 4. Electronic spectra of **3a** and its reduced species.

reduction state generated by applying constant voltage corresponding to the formation of $\mathbf{3a}^{\bullet-}$, $\mathbf{3a}^{2-}$, $\mathbf{3a}^{3\bullet-}$, and $\mathbf{3a}^{4-}$.[17] Their absorption maxima are summarized in Table 2. The electronic absorption spectrum of $\mathbf{3a}^{\bullet-}$ exhibited four maxima at 457, 658, ca. 1200, and 1457 nm in the vis–NIR region. The DFT calculation predicted that the first excited state was found at 1.04 eV (1189 nm), and the transition to this state corresponded to the CR band, which associates with a one-electron transition from the SOMO to the LUMO that occurs mainly at the DCF

Table 2. Comparison of Experimental (3a) and Calculated Absorption Maxima (3b)

charge	exptl[a] (**3a**) λ_{max} [nm]	calcd[b] (**3b**) λ_{max} [nm]
−1	457, 658, 1200,[c] 1457	352, 615, 1020, 1189
−2	315, 920	401, 788
−3	445, 1195	566, 1054
−4	443, 672	506, 628

[a]In THF solution. [b]TD-(U)B3LYP/6-311++G(d,p)//(U)B3LYP/6-311++G(d,p). [c]Shoulder absorption.

moieties.[18] This result clearly supports the stable mixed-valence state that resulted from the delocalization of the anionic charge between two $(CN)_2C=$ units through the *s*-indacene core in $\mathbf{3a}^{\bullet-}$. In sharp contrast, the CR band disappeared in $\mathbf{3a}^{2-}$. An intensive absorption band at 920 nm was observed in $\mathbf{3a}^{2-}$. In the DFT calculation for $\mathbf{3b}^{2-}$, a planar *s*-indacene π-core with a biradical anionic character, estimated by the natural orbital occupation number method,[19] was found to be the minimum energy geometry. The TD-DFT suggested an electron transition at 788 nm as the lowest energy band corresponding to the HOMO–LUMO transition of the 12π-electron *s*-indacene core. In the electronic spectra of $\mathbf{3a}^{3\bullet-}$, another CR band appeared at 1195 nm, reflecting its open-shell electronic structure owing to further reduction from the *s*-indacene core. The TD-DFT calculation for $\mathbf{3b}^{3\bullet-}$ also reproduced the CR band at a lower energy region. The optimized geometry suggested a contribution of an anionic *s*-indacene moiety. In the spectrum of $\mathbf{3a}^{4-}$, there were distinctive absorptions only in the UV–vis region.

Finally, we prepared anionic species chemically. The slow evaporation of a mixed solution of **3a** and 2 equiv of cobaltocene ($CoCp_2$) as the reducing agent gave a single crystal of $\mathbf{3a}^{2-}\cdot 2(CoCp_2)$, which was subjected to X-ray analysis. As shown in Figure 5, the crystal lattice contains **3a** and two different $CoCp_2$

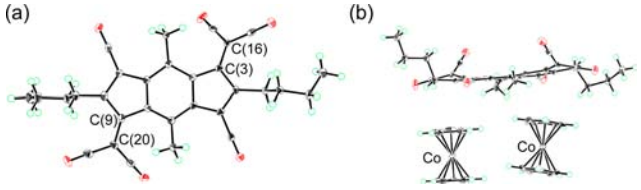

Figure 5. ORTEP drawing of $\mathbf{3a}\cdot(CoCp_2)_2$. (a) Top View. (b) Side view with cobaltocenium ion.

molecules, forming a mixed-stack CT complex. In addition, the electronic spectrum of the crystals in MeCN was quite similar to that of $\mathbf{3a}^{2-}$ that was generated electrochemically (Figure S7). As with the crystal structure of the neutral species, $\mathbf{3a}^{2-}$ also adopted a distorted form at the $C(CN)_2$ moieties. The lengths of the exocyclic C(3)–C(16) and C(9)–C(20) bonds were 1.437 and 1.439 Å, respectively, which were longer than those of C(5)–C(8) of **3a** (1.370 Å). A deformation was observed in comparison to the central six-membered core of the neutral structure. The harmonic oscillator model of aromaticity (HOMA) value for the central benzene ring was calculated to be 0.670 for $\mathbf{3a}^{2-}$, while the HOMA value of **3a** was found to be 0.915. These facts implied the substantial loss of the aromatic character of the central ring of $\mathbf{3a}^{2-}$. In addition, clear bond alternation was found at the five-membered rings of the DCF moieties. Moreover, calculations of NICS(0) (estimated by HF/6-311++G(d,p)) are also consistent with the trends: a negative value of −6.37 and a positive value of +4.82 ppm were obtained for **3a** and $\mathbf{3a}^{2-}$, respectively. These results clearly suggested contribution of the *s*-indacene structure to the dianionic state.

In summary, we have synthesized 1,5-dihydro-*s*-indacene with six CN groups as a novel electron-accepting molecule. This may be a promising candidate for electron transporting n-type materials. The removal of the benzo-annulation from the conventional indenofluorene framework successfully led to a facile reduction. The CV of **3a** exhibited four reversible redox waves, and the absorption spectra and UPS spectra revealed a fairly low-lying LUMO energy level. The electronic structures of $\mathbf{3a}^{n-}$ ($0 < n < 4$) were investigated using electrospectrochemistry.

dx.doi.org/10.1021/ol502675n | *Org. Lett.* 2014, 16, 5608–5611

The intensive CR band was observed in the open-shell species. In addition, the X-ray structure of the CT-complex of $\mathbf{3a}^{2-}$ clearly suggested an *s*-indacene core.

■ ASSOCIATED CONTENT

Supporting Information

Experimental details of the synthesis; NMR chart; UV absorption of **5**, **6**, and **3a**; details of the X-ray analysis, UPS measurements, and DFT calculations. This material is available free of charge via the Internet at http://pubs.acs.org.

■ AUTHOR INFORMATION

Corresponding Authors

*E-mail: masasi.h@kitasato-u.ac.jp.
*E-mail: mazaki@kitasato-u.ac.jp.

Notes

The authors declare no competing financial interest.

■ ACKNOWLEDGMENTS

We thank Prof. Dr. Takahiro Tsuchiya (Kitasato University) for helpful discussions. All calculations were performed at the Research Center for Computational Science, Okazaki, Japan.

■ REFERENCES

(1) (a) Anthony, J. E. *Chem. Rev.* **2006**, *106*, 5028. (b) Takimiya, K.; Kunugi, Y.; Otsubo, T. *Chem. Lett.* **2007**, *36*, 578. (c) Murphy, A. R.; Fréchet, J. M. J. *Chem. Rev.* **2007**, *107*, 1066.

(2) (a) Newmann, C. R.; Frisbie, C. D.; Da Silva Filho, D. A.; Brédas, J.-L.; Ewbank, P. C.; Mann, K. R. *Chem. Mater.* **2004**, *16*, 4436. (b) Jung, B. J.; Tremblay, N. J.; Yeh, M.-L.; Katz, H. E. *Chem. Mater.* **2011**, *23*, 568. (c) Wen, Y.; Liu, Y. *Adv. Mater.* **2010**, *22*, 1331.

(3) (a) Kawase, T.; Konishi, A.; Hirao, Y.; Matsumoto, K.; Kurata, H.; Kubo, T. *Chem.—Eur. J.* **2009**, *15*, 2653. (b) Zhang, H.; Karasawa, T.; Yamada, H.; Wakamiya, A.; Yamaguchi, S. *Org. Lett.* **2009**, *11*, 3076. (c) Levi, Z. U.; Tilley, T. D. *J. Am. Chem. Soc.* **2010**, *132*, 11012.

(4) (a) Hafner, K. *Pure. Appl. Chem.* **1982**, *54*, 939. (b) Hafner, K.; Stowasser, B.; Krimmer, H.-P.; Fischer, S.; Böhm, M. C.; Lindner, H. J. *Angew. Chem., Int. Ed. Engl.* **1986**, *25*, 630. (c) Cary, D. R.; Green, J. C.; O'Hare, D. *Angew. Chem., Int. Ed. Engl.* **1997**, *36*, 2618.

(5) (a) Zhou, Q.; Carroll, P. J.; Swager, T. M. *J. Org. Chem.* **1994**, *59*, 1294. (b) Chase, D. T.; Rose, B. D.; McClintock, S. P.; Zakharov, L. N.; Haley, M. M. *Angew. Chem., Int. Ed.* **2011**, *50*, 1127. (c) Chase, D. T.; Fix, A. G.; Rose, B. D.; Weber, C. D.; Nobusue, S.; Stockwell, C. E.; Zakharov, L. N.; Lonergan, M. C.; Haley, M. M. *Angew. Chem., Int. Ed.* **2011**, *50*, 11103. (d) Rose, B. D.; Sumner, N. J.; Filatov, A. S.; Peters, S. J.; Zakharov, L. N.; Petrukhina, M. A.; Haley, M. M. *J. Am. Chem. Soc.* **2014**, *136*, 9181.

(6) (a) Chase, D. T.; Fix, A. G.; Kang, S. J.; Rose, B. D.; Weber, C. D.; Zhong, Y.; Zakharov, L. N.; Lonergan, M. C.; Nuckolls, C.; Haley, M. M. *J. Am. Chem. Soc.* **2012**, *134*, 10349. (b) Nishida, J.; Tsukaguchi, S.; Yamashita, Y. *Chem.—Eur. J.* **2012**, *18*, 8964.

(7) (a) Shimizu, A.; Kubo, T.; Uruichi, M.; Yakushi, K.; Nakano, M.; Shiomi, D.; Sato, K.; Takui, T.; Hirao, Y.; Matsumoto, K.; Kurata, H.; Morita, Y.; Nakasuji, K. *J. Am. Chem. Soc.* **2010**, *132*, 14421. (b) Shimizu, A.; Kishi, R.; Nakano, M.; Shiomi, D.; Sato, K.; Takui, T.; Hisaki, I.; Miyata, M.; Tobe, Y. *Angew. Chem., Int. Ed.* **2013**, *52*, 6076. (c) Shimizu, A.; Tobe, Y. *Angew. Chem., Int. Ed.* **2011**, *50*, 6906. (d) Kubo, T.; Shimizu, A.; Sakamoto, M.; Uruichi, M.; Yakushi, K.; Nakano, M.; Shiomi, D.; Sato, K.; Takui, T.; Morita, Y.; Nakasuji, K. *Angew. Chem., Int. Ed.* **2005**, *44*, 6564.

(8) Frank, W.; Gompper, R. *Tetrahedron Lett.* **1987**, *28*, 3083.

(9) (a) Usta, H.; Facchetti, A.; Marks, T. J. *Org. Lett.* **2008**, *10*, 1385. (b) Usta, H.; Facchetti, A.; Marks, T. J. *J. Am. Chem. Soc.* **2008**, *130*, 8580. (c) Usta, H.; Risko, C.; Wang, Z.; Huang, H.; Deliomeroglu, M. K.; Zhukhovitskiy, A.; Facchetti, A.; Marks, T. J. *J. Am. Chem. Soc.* **2009**, *131*, 5586.

(10) (a) Andrew, T. L.; Cox, J. R.; Swager, T. M. *Org. Lett.* **2010**, *12*, 5302. (b) Andrew, T. L.; Bulović, V. *ACS Nano* **2012**, *6*, 4671.

(11) Adams, C.; Araneda, J.; Morales, C.; Chavez, I.; Manriquez, J. M.; Carey, D. M.-L.; Katir, N.; Castel, A.; Riviére-Baudet, M.; Dahrouch, M.; Gatica, N. *Inorg. Chim. Acta* **2011**, *366*, 44.

(12) (a) Harusawa, S.; Yoneda, R.; Kurihara, T.; Hamada, Y.; Shiori, T. *Chem. Pharm. Bull.* **1983**, *31*, 2932. (b) Harusawa, S.; Yoneda, R.; Kurihara, T.; Hamada, Y.; Shioiri, T. *Tetrahedron Lett.* **1984**, *25*, 427.

(13) Youngman, M.; Kazmierski, W. M.; Yang, H.; Aquino, C. J. (Smithkline Beecham Co., USA). Preparation of Indane compounds and analogs as CCR5 antagonists. US Patent WO 2004055012, 2004.

(14) For further details, see Supporting Information.

(15) All calculations were performed using Gaussian 09, Revision D.01. Frisch, M. J. et al. Gaussian, Inc.: Wallingford, CT, 2009. See the Supporting Information for the full citation.

(16) Hill, I. G.; Kahn, A.; Soos, Z.; Pascal, R. A., Jr. *Chem. Phys. Lett.* **2000**, *327*, 181−188.

(17) The voltages at −0.50, −1.50, −2.0, and −3.0 V in Figure 4 indicated E_{pc} values vs Fc/Fc^{+}, using a Pt mesh working electrode, that correspond to the formation of each anionic species, respectively.

(18) Hasegawa, M.; Takatsuka, Y.; Kuwatani, Y.; Mazaki, Y. *Tetrahedron Lett.* **2012**, *53*, 5385.

(19) Döhnert, D.; Koutecky, J. *J. Am. Chem. Soc.* **1980**, *102*, 1789.